Journal of Asian Ceramic Societies

ISSN: (Print) (Online) Journal homepage: https://www.tandfonline.com/loi/tace20

The effect of sintering regime on superhydrophobicity of silicon nitride modified ceramic surfaces

Gokhan Acikbas & Nurcan Calis Acikbas

To cite this article: Gokhan Acikbas & Nurcan Calis Acikbas (2021) The effect of sintering regime on superhydrophobicity of silicon nitride modified ceramic surfaces, Journal of Asian Ceramic Societies, 9:2, 734-744, DOI: 10.1080/21870764.2021.1915563

To link to this article: https://doi.org/10.1080/21870764.2021.1915563

Published online: 15 Apr 2021.

JOURNAL OF ASIAN CERAMIC SOCIETIES
2021, VOL. 9, NO. 2, 733–743
https://doi.org/10.1080/21870764.2021.1915563

THE CERAMIC SOCIETY OF JAPAN
THE KOREAN CERAMIC SOCIETY
Taylor & Francis
Taylor & Francis Group

FULL LENGTH ARTICLE

The effect of sintering regime on superhydrophobicity of silicon nitride modified ceramic surfaces

Gokhan Acikbas[a] and Nurcan Calis Acikbas[b]

[a]Bilecik S.E. University, Mechanical and Metal Technologies Department, Bilecik, Turkey; [b]Department of Metallurgical and Materials Engineering, Mersin University, Engineering Faculty, Mersin, Turkey

ABSTRACT

The most common method of obtaining a superhydrophobic surface is to create a specific surface morphology and then coat it with a hydrophobic polymer. Numerous such morphological surfaces have been developed but are often fragile. Ceramic-based coatings show longer life with high wear resistance. In this study, surface micro-nano surface morphology was developed with β-Si_3N_4 powder and the influence of sintering regime on contact angle of ceramic surfaces was investigated. The contact angle, surface energy and surface roughness were determined from the developed surfaces and surface morphology analyzed by scanning electron microscopy, phase evolution was determined by X-Ray diffraction. Changes in sintering regimes lead to different phase evolutions, roughness, surface topography, surface free energies and contact angles. The superhydrophobicity resulted mainly due to the surface structure/topography in the micro-nano hybrid structures of β-Si_3N_4 crystals. The highest water contact angle achieved was 166° of the samples sintered at 980°C for 5 min.

ARTICLE HISTORY
Received 29 January 2021
Accepted 08 April 2021

KEYWORDS
Si_3N_4; superhydrophobicity; sintering; micro-nano hybrid structures; ceramic surfaces

1. Introduction

The wettability of a surface is defined by the ability of a liquid droplet to spread over a solid surface and is governed by its microstructural features and chemical properties of surfaces. Hydrophobicity is usually determined by measuring the angle of the water droplet after contact with a solid surface. If the water contact angles are higher than 150°, these surfaces are called superhydrophobic. Up to now, many studies have been conducted on superhydrophobic surfaces. Studies conducted by Johnson and Dettre can be considered as the first studies about the superhydrophobic surfaces [1]. Despite the fact that superhydrophobic term was not used, the principles of the superhydrophobic state were presented. It was disclosed that the principle of this hypothesis was based on the surface roughness, surface chemistry and contact angle hysteresis.

The superhydrophobic nature, which affects self-cleaning surfaces, is of scientific and industrial interest. This advanced water repellence feature finds many applications in industry and daily life such as a mirror surface that does not steam up, waterproof mobile phones, aircraft wings, textile products, etc. Some naturally occurring surfaces, such as lotus leaves and snail shells, have self-cleaning properties. Owing to the superhydrophobic feature, when the surface is slightly tilted, water drops rotate on the surface and move, and thereby dirt on the surfaces is cleaned. How the lotus leaf exhibits this feature was explained by means of the electron microscope studies conducted on the biological surfaces in the end of the 1970s. A rough surface coated with the wax of the lotus leaf contains epidermal cells. Wax crystals provide a hydrophobic layer and increase surface roughness according to the Wenzel and Cassie Baxter models. Wetting feature of the wax crystals is very poor. As a result, a water drop on the surface minimizes the interaction between the surface and itself. In this way, a spherical drop is formed on the surface. Since the dirt on the leaf surface is bigger than the cellular structure of the leaf, particles on the surface protrusions can be removed from the surface. Consequently, interaction between the contact area and the interface is minimized. On the other hand, surfaces having surface contact angle higher than 150° were obtained; however, there exist studies in which the drop does not roll on when it was tilted. This indicates that even if a contact angle of 150° is provided, sufficient superhydrophobicity is not provided, since the surface hysteria is not decreased. Hysteria means the difference between the angles of progress and separation directions of the drop on the solid surface, and this value provides a superhydrophobic feature only when it is degraded to a minimum value [2]. Until now, many methods have been reported for obtaining superhydrophobic surfaces by mimicking the surface of lotus leaves [3–13]. However, all these methods are subject to

CONTACT Nurcan Calis Acikbas ncalis@gmail.com Mersin University, Engineering Faculty, Metallurgical and Materials Engineering Department, Mersin 33343, Turkey.

certain limitations like longevity, being expensive, poor mechanical durability of surfaces, etc.

In literature there are some studies to obtain superhydrophobicity on ceramic surfaces [14–18]. Cacciotti et al. produced SiO_2 coatings on glazed sanitarywares via a spraying technique based on TEOS and MTES as precursors. They stated this application provided improvement of the hydrophobicity and stain resistance of the glazed sanitarywares. However, the obtained maximum water contact angle was 90º [14]. Reinosa and coworkers obtained hydrophobic properties with a contact angle of 115º with the addition of copper in the glaze [15]. Määttä et al. studied the cleanability property of ceramic sanitarywares by coating with a sol–gel-derived titania and zirconia. The studies revealed that the coatings had little effect on contact angle but these coatings affected the cleanability of ceramics in a positive way. The obtained maximum water contact angle was 97º [16]. Kuisma et al. investigated the effect of titania and zirconia coatings on cleanability of ceramic tile surfaces. They showed that titania coatings gave increased cleanability than zirconia coating and the obtained maximum water contact angle was between 80º-90º [17]. Up to now maximum contact angle of 150º was achieved with addition of metallic zinc powder into ceramic wall tile glaze mixture [18].

Hierarchical surface structure together with the hydrophobic chemistry shows superhydrophobicity. Silicon nitride-based ceramics with hierarchical structures attracted interest in the scientific world in recent years [19]. However, there are very limited studies on the surface energy of silicon nitride-based ceramics in literature. Rosso showed that water contact angles (θ) of Si_xN_4 substrates modified by different 1-alkenes and 1-alkynes are maximum 108° [20]. In this paper, the four different sintering regimes were applied to get superhydrophobic ceramic surfaces with β-Si_3N_4 powder. Superhydrophobic surface properties were compared taking into account the phase evolution, microstructure as well as the wettability and surface energies correlated with of the surfaces depending on the sintering regimes.

2. Material and methods

2.1. Starting materials

The substrate is an industrial ceramic wall tile 3 × 3 cm in size and taken from Bien Ceramic Factory, Bilecik. In order to obtain the superhydrophobicity the combustion synthesized beta silicon nitride (β-Si_3N_4) powder (Beijing Chanlian-Dacheng Trade Co. Ltd., China) was used as an additive for wall tile glaze mixture. Since the Si_3N_4 phase has high decomposition temperature (1877°C) and non-melted at the maturing temperature of wall tile glaze, it is selected to achieve micro-nano surface morphology [21]. The β-Si_3N_4 powder has 0.50 µm of the mean particle size, 29.21 m^2/g surface area and have β-$Si_3N_{4\%}$100 crystalline phase.

2.2. Preparation of β-Si_3N_4 Rich Glaze Mixture

Before the β-Si_3N_4 powder is added to the glaze slurry, the particle size of industrial wall tile glaze was down to 1 µm. Because we previously observed that coarse starting particle size (10 µm ≤) couldn't provide desired surface topography for obtaining superhydrophobicity [22,23].

Thus, the average particle size was down to 1 µm after 16 hours milling (see Figure 1). Milling was carried out with planetary mill at 400 rpm using silicon nitride balls (ϕ: 3 mm), since planetary mill has higher efficiency than ball mill. Sodium tripolyphosphate (Euro Kimya, Turkey) was used as a dispersant (0.25%).

After that 67 wt% β-Si_3N_4 powder was added into wall tile glaze slurry and mixed with jet mills rotated at 120 rpm for 20 min with a milling load of alumina balls and in water medium with 35% water and 65% dry matter (Frit, China clay, β-Si_3N_4 powder), 3 ppt sodium carboxymethyl cellulose (Lamberti) and 1.5 ppt sodium tripolyphosphate (Euro Kimya, Turkey). The glaze formulation was, frit (boric acid 15%, alumina 3%, quartz 27%, potassium feldspar 35%, potassium nitrate 2%, calcite 15%, magnezite 3%,3 ppt sodium carboxymethyl cellulose, 1.5 ppt sodium tripolyphosphate), 5% china clay, and 67% β-Si_3N_4 powder, all

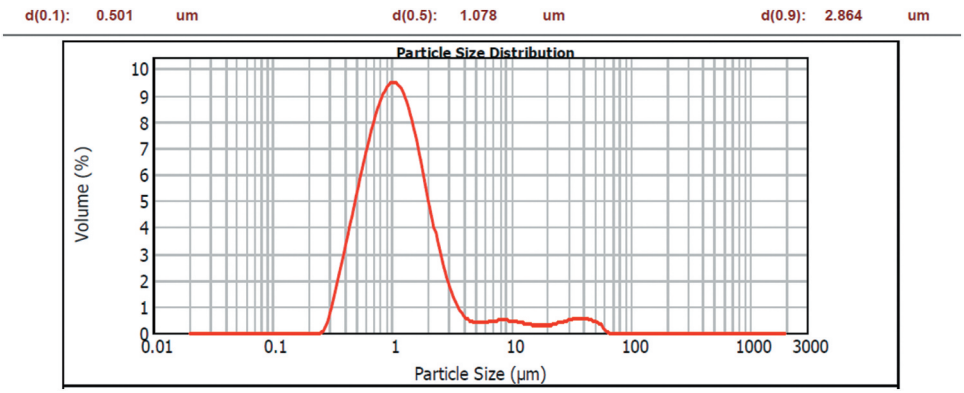

Figure 1. The particle size distribution graph of wall tile glaze after 16 hours milling.

percentages being by weight. The glaze slurry was sieved through 45 μm. The liter weight of modified glaze is 1820 g/L and fordcup viscosity is 30 s.

2.3. Characterization of glaze-melting behavior with hot stage microscopy

The effect of particle size reduction of industrial wall tile glaze on thermal behavior of glaze and to determine sintering temperature was investigated with hot stage microscopy technique (HSM type 3 M, Misura). The hot stage microscope regime has a heating rate of 50°C/min to 400°C then with 10°C/min with heating rate from 400°C to 1200°C.

2.4. Firing

The ceramic substrates coated with glaze rich in β-Si_3N_4 powder were sintered in a laboratory muffle kiln (MagmaTherm, Tetra, Turkey) at the different sintering regimes: 980°C for 5 min., 1050°C for 60 min. and 1100°C for 5 and 60 min. with a heating rate of 30◦C/min below 500◦C and 5◦C/min above 500◦C and natural cooling in the furnace cooling rate of ~5◦C/min. Firing temperature was selected taking into account hot stage microscopy results and the sintering temperature was chosen below 1128°C in order to avoid bloating problem. In order to check reproducibility, the samples were sintered three times in laboratory furnace and five samples sintered at each run.

2.5. Coating with polymer

Since the sintered ceramic surfaces were porous, the surfaces were coated with polymers to prevent water absorption. The ceramic substrates were heated at 120°C for 10 minutes before spray coating with polymer. Commercial polymeric composition of 10% fluoropolymer, 60% alkoxysilane and 30% ethanol, under the trade name ECC-4000. The sprayed quantity was approximately 250 g/m^2.

2.6. Surface characterization techniques

The modified glaze surfaces were analyzed by the X-ray diffraction technique (XRD-Panalytical, Empyrean) to determine the types of crystalline phases (2θ between 10° and 60° with a scan rate of 2°/min). The surface morphology of the modified surfaces was examined by a scanning electron microscope (SEM-ZEISS Supra 40VP) by using the secondary electron imaging mode. A Mitutoyo SJ-301 surface roughness tester was used to measure the surface roughness of the modified ceramic tile surfaces. Arithmetic mean deviation of the troughs and crests from the mean line of the roughness profile (Ra) were recorded as roughness parameters. The drop shape analyzer (Kruss, DSA-25) was used to determine contact angle and surface free energy (SFE) values by using water and diiodomethane as liquids with 5 μl drops. The SFE calculations were done according to Young's equation and a two-component model developed by Fowkes [24] and Owens, Wendt, Rabel and Kaelble (OWRK method) [25,26]. Detailed descriptions of the calculations were given in our previous paper [18].

3. Results and discussion

3.1. Determination of sintering regimes

The hot stage microscopy curve displays the dimensional variations versus the temperature of compacted glaze powders with different average particle sizes (10 and 1 μm). The softening, half-sphere and fusion temperatures are very close for both glazes (Figure 2) since the glaze composition consisted of 67% Si_3N_4, which is high refractory (Tdecomposition: 1877°C). Indeed, according to Herring's scaling law, it is expected that smaller particle size accelerates the sintering when the powders are similar shapes and sintered by the same sintering mechanism [27]. We did not however observe this effect since the glaze composition consisted of 67% Si_3N_4, which is high refractory (Tdecomposition: 1877°C).

According to the graphic, sintering started at 858°C and 874°C, softening temperatures are 1076°C and 1068°C, half sphere temperatures are 1116°C and 1106°C, fusion temperatures are 1128°C and 1188°C for glazes with average particle size of 10 μm and 1 μm, respectively. It is seen from the graphic, Si_3N_4 modified glazes spread above 1128°C (d_{50}: 1 μm), and 1188°C (d_{50}: 10 μm). Therefore firing temperatures were chosen below 1128°C. According to hot stage microscopy graphic, bloating problem may be observed above 1128°C (d_{50}: 1 μm) and 1188°C (d_{50}: 10 μm).

3.2. Surface properties

The ceramic surfaces coated with Si_3N_4 rich glaze have matte feature and crack free. The micro-roughness of these surfaces has been measured by a value of Ra between 140 and 487 μm depending on applied sintering regime. On the other hand, the measured industrial glaze surface roughness was 2 μm without β-Si_3N_4 addition. The roughness of surfaces was at its maximum value 487 μm for the sample sintered at 1050°C for 60 min. With an increase in sintering temperature from 1050°C to 1100°C, the surface roughness was down to 140 μm. After all sintering regimes, the surface was matte, except the sample sintered at 1100°C for 60 minutes. The results showed that both peak temperature and dwell time of sintering have an effect on surface roughness. With an increase in sintering

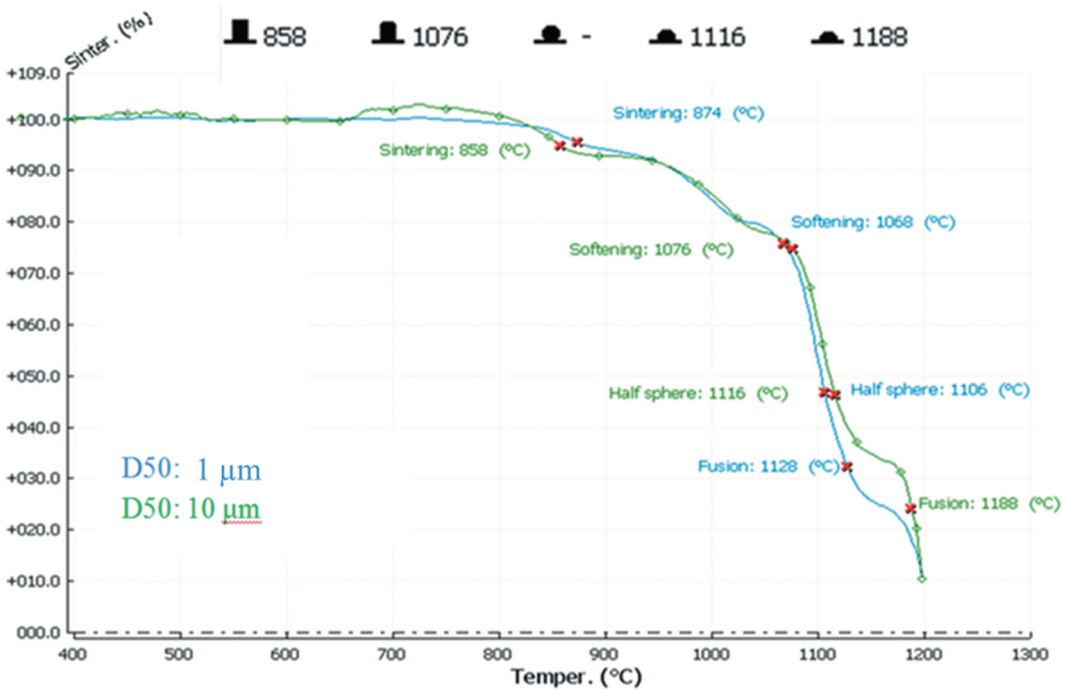

Figure 2. The hot stage microscope curves of Si_3N_4 added industrial and milled glaze.

temperature from 980°C to 1100°C (5 min), surface roughness increases. With the increase in sintering time from 5 to 60 minutes at 1100°C, surface roughness decreased from 352 to 140 µm and the surface feature had changed from matte to bright. This phenomenon is related to crystallization and phase evolutions.

The XRD spectra of the samples sintered at different sintering regimes are compared in Figure 3. β: (beta Silicon nitride, β-Si_3N_4), Z: (Zircon, $ZrSiO_4$), Q: (Quartz, SiO_2), D: (Diopside, $CaMgSi_2O_6$), A: (Anorthite, $CaAlSi_2O_8$) and C: (Cristobalite, SiO_2) phases are detected by XRD analysis. The highest Z peak intensity was obtained with the samples sintered at 1100°C for 60 min (2θ: 27.01, I_{max}:100). The second highest intensity Z peak was acquired when the samples were sintered at 980°C for 5 min. The Z peak intensity is weaker when the samples are sintered at 1100°C for 5 min and 1050°C for 60 min. β peak intensity is high in all surfaces which sintered at different sintering regimes.

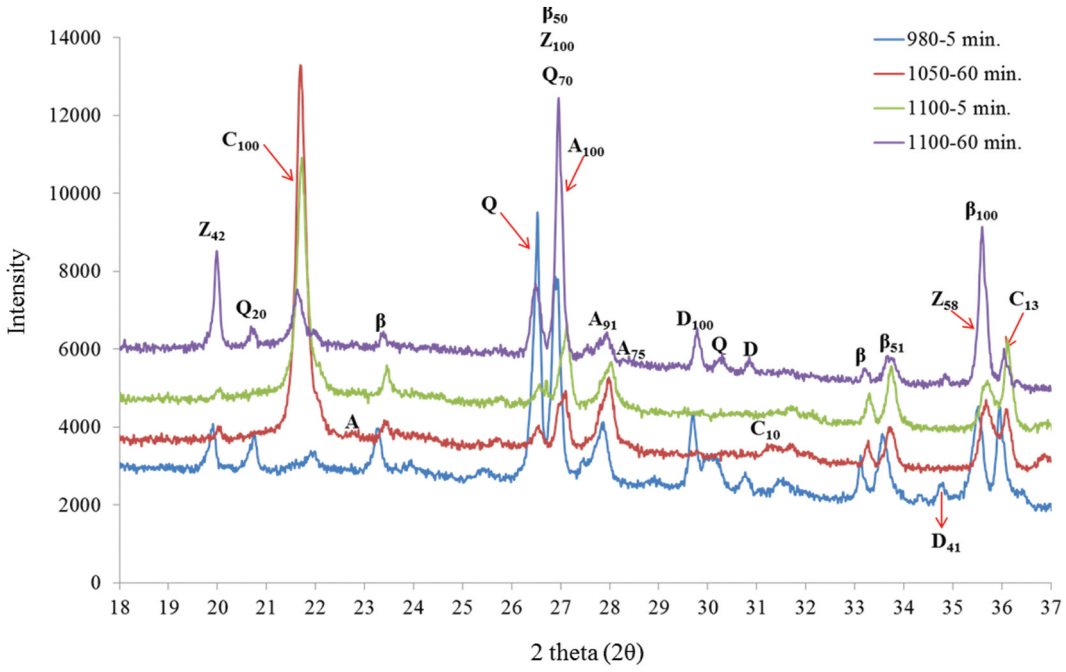

Figure 3. XRD graph of ceramic surfaces coated with Si_3N_4 rich glaze (β: β-Si_3N_4, Z: Z, A: A; Q: Q, C: C, D: D; numbers state peak intensities).

When the samples were sintered at 980°C for 5 min, the highest Q phase intensity was attained. The Q phase has no adverse effect on superhydrophobicity since these surfaces have high contact angle (166°). For all other sintering regimes, Q peak intensity is weak compared to samples sintered at 980°C. The lowest Q peak intensities were observed when the samples were sintered at 1100°C for 5 min and 1050°C for 60 min. The A peak intensities are mostly weak in all samples compared to other phases. The highest A peak intensity was observed when the sample was sintered at 1050°C for 60 min. The samples have similar A peak intensity sintered at 980°C for 5 min and 1100°C for 5 min. The highest D peak was attained when the samples were sintered at 980°C for 5 min. For the samples sintered at 1100°C for 60 min the D peak intensities were high. After sintering at 1050°C for 60 min and 1100°C for 5 min, the D peak was not observed. The highest C peak intensities were observed when the samples were sintered at 1050°C for 60 min. and 1100°C for 5 min. Since the thermal expansion coefficient of C is very high ($\alpha_{25\text{-}200oC}$:$20x10^{-6}$ K^{-1}), a crazing problem may be observed on glaze (α_{glaze} □ α_{body}) with time [28]. According to XRD results, there is no relation between Z peak intensity and contact angle since the samples sintered at 1100°C for 60 min has the highest Z peak intensity with a lowest contact angle (68°) and the samples sintered at 980°C for 5 min have very strong Z peaks with a highest contact angle (166°). In literature there are no data available on the contact angle or surface energy of Z. Surface with 166° contact angle has strong Q peaks. The contact angle of Q was stated as maximum 50° in literature [29]. Therefore the superhydrophobicity of the surfaces is directly related to β phase.

As mentioned, the highest peak intensity of β phase is ~36° and C is ~21.7°. C phase was not observed when the samples were sintered at 980°C for 5 min and β phase peak intensity is high. This indicates that Si_3N_4 does not oxidize in this sintering regime. In literature, it was stated that an Si-N bond is chemically reactive and should oxidize when exposed to air [30]. But, the kinetics of nitride surface oxidation is slow at lower temperatures. Little is known about nitride reactivity at lower temperatures. And any oxynitride phase formation was not observed in our XRD analysis. Raider and coworkers stated that an oxidized film is present at a silicon nitride surface after oxidation at 1070°C in dry oxygen [30]. Binding-energy data indicate that silicon dioxide is not a major component of the oxidized film unless the nitrides are oxidized for more than 1 hr. The film formed after oxidation for one-half hour is mainly oxynitride on silicon nitride, with no evidence of the presence of significant silicon dioxide. On the other hand, the surfaces have similar C and β phase peak intensities when the sintering regimes are 1050°C for 60 min and 1100°C for 5 min. When the sintering temperature was 1100°C and dwell time was 60 min, β phase peak intensity decreases to half height of others and C phase peak intensity is lower than the sintering regimes are 1050°C for 60 min. and 1100°C for 5 min. If the Si_3N_4 was not stable and oxides, the highest C phase peak intensity would be observed at 1100°C and dwell time was 60 min. In SEM images (Figure 10) bloating was observed when the sintering time increased to 60 min due to oxidation of Si_3N_4 but it is not too much.

The wettability of the surface depends on surface energy and surface roughness. Although all surfaces are coated with polymer, different surface energies have been obtained due to different surface morphologies. This result proved that the contact angle of the surface is influenced by the surface morphology rather than the polymer coating. This proves that superhydrophobicity is due to the micro/nano hybrid surface topography not related to the surface chemistry directly. The thin polymer coating mimics the surface topography of the Si_3N_4 surface beneath it therefore it too provides superhydrophobic effect. The polymer coating was applied on purpose to avoid the water to be absorbed by the porous Si_3N_4 layer. The similar results were declared in literature [18]. In our previous study, we used metallic micro-grade zinc powder to obtain superhydrophobic surface. The water contact angle of 150° was achieved when the samples sintered at 1000 ◦C peak temperature due to the formation of micro–structured nanocrystalline zinc oxide granules providing a specific surface topography. At higher peak temperatures the hydrophobicity was lost as the specific granular surface topography deteriorated with the conversion of zinc oxide granules to the ubiquitous willemite crystals. However, the gloss fired tiles with the zinc modified glaze but without the polymeric coating, even though the initial contact angles were large, completely absorbed the water droplet, the contact angle dropping to zero in a few minutes. This phenomenon was due to the fact that the zinc modified glaze did not vitrify enough to provide a glassy surface at none of the heat treatment temperatures. The sintered granular surface structure was porous absorbing water. The polymer coating on the ceramic tile surfaces functioned only as a water impermeable layer, and the induced hydrophobicity was due to the particular surface topography generated by the nanocrystalline zinc oxide granules rather than the chemical structure of the surface. In our case, for a sintering temperature between 980°C and 1050°C and a dwell time between 5 and 60 minutes, the contact angles of formed surface are superhydrophobic (154-166°). When the dwell time was 60 minutes and the sintering temperature was 1100°C, the contact angle dropped abruptly to 68° and showed a hydrophilic character. This phenomenon can be related mainly due to surface morphology. The surface morphology affects the surface energy rather than polymer coating.

The detailed microscopic investigations of the developed surfaces were carried out. All sintered surfaces are porous and water retentive, as shown by the SEM images given in Figure 4. It is evident that in all cases the surfaces were crack-free and remarkably rougher due to the characteristic irregularities. These rough textured surfaces provide high contact angles. The incorporation of the Si_3N_4 powder in the glaze results in the development of micro-nano scale hybrid surface topography. It has also been verified that the sintering temperature and dwell time affect the surface morphology (roughness, porosity content and pore size).

When the samples were sintered at 980°C and 1050°C, the surface has a ball-like spherical granular structure with a diameter of 5-20 µm and nano–whiskers on these balls. The surface topographies formed naturally resemble a super hydrophobic lotus flower leaf. These surfaces have low surface energies 1.3 and 1.58 mJ/m^2 and very high water contact angles (166° and 154°). By increasing sintering temperature to 1100°C, these spherical balls disappear. As the sintering temperature and time increase, porosity content and pore size increase. For the samples sintered at 980°C for 5 min., the porosity content is low compared to other surfaces and the pore size changes between 0.5 µm to 1 µm. When the sintering temperature increases to 1050°C, porosity content and pore size increase and reache 5–20 µm due to increased temperature. At a constant sintering temperature of 1100°C for different sintering times (5 and 60 min.), porosity content and size show differences. For instance, when the sintering time was 5 min., the surface had high porosity content and pore sizes change within a wide range (1–20 µm). When the sintering time is extended to 60 min., pore sizes are getting bigger and reach 10–50 µm since longer dwell time.

The SEM images in Figure 5 show that the surfaces have high contact angles (166°) obtained at 980°C for 5 min. The surface has relatively low porosity and pore sizes are small (0.5-1 µm). The surface has a ball–like spherical granular structure with a diameter of 5-15 µm (Figure 6). When images were taken at high magnifications (50,000x), nano scale whiskers were seen on the ball-like granules. On the other hand, very fine crystals (50–200 nm) were observed in other regions (see Figure 6c). These types of surface structures can be attributed to super-hydrophobicity. The EDX spectra of spherical balls are given in Figure 6d. This contains silicon, nitrogen, oxygen, zirconium, aluminum, calcium and sodium elements. This showed that the balls are mainly silicon nitride but contain other elements in the starting composition. During firing, silicon nitride phase reacts with the other starting materials and this kind of spherical balls form. In the partially molten state the viscosity of the Si_3N_4 rich phase is higher than the surrounding partially liquid phases, causing the observed phenomenon of the sphere-like agglomeration of the Si_3N_4 phase.

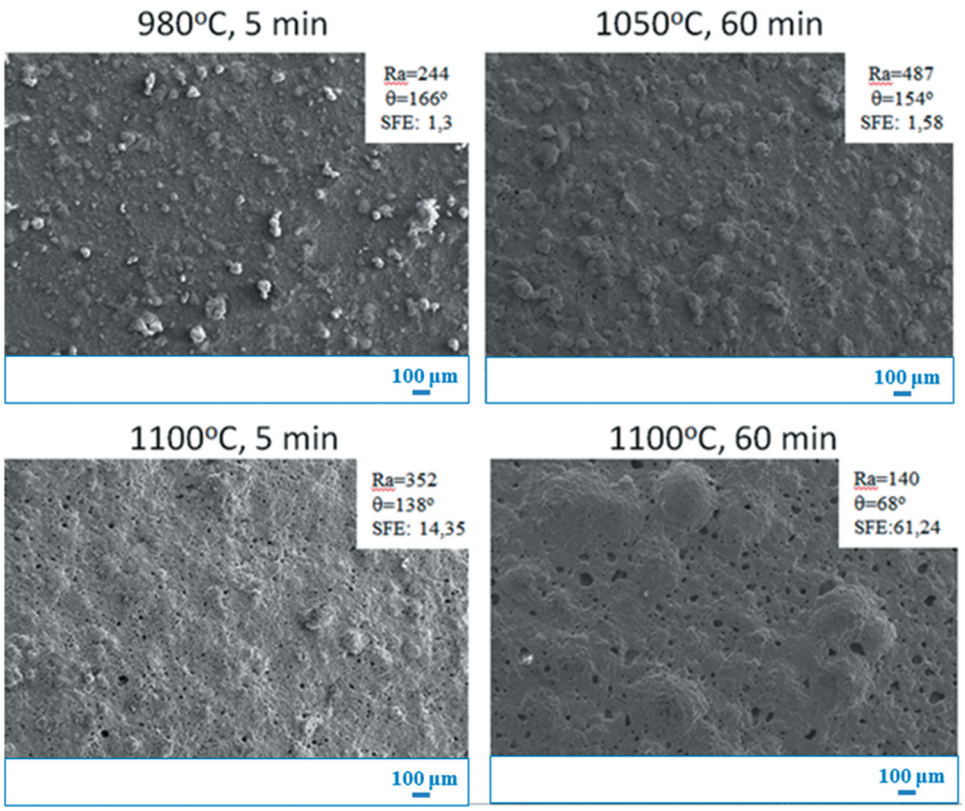

Figure 4. The SEM-SE images of samples sintered at different sintering regimes.

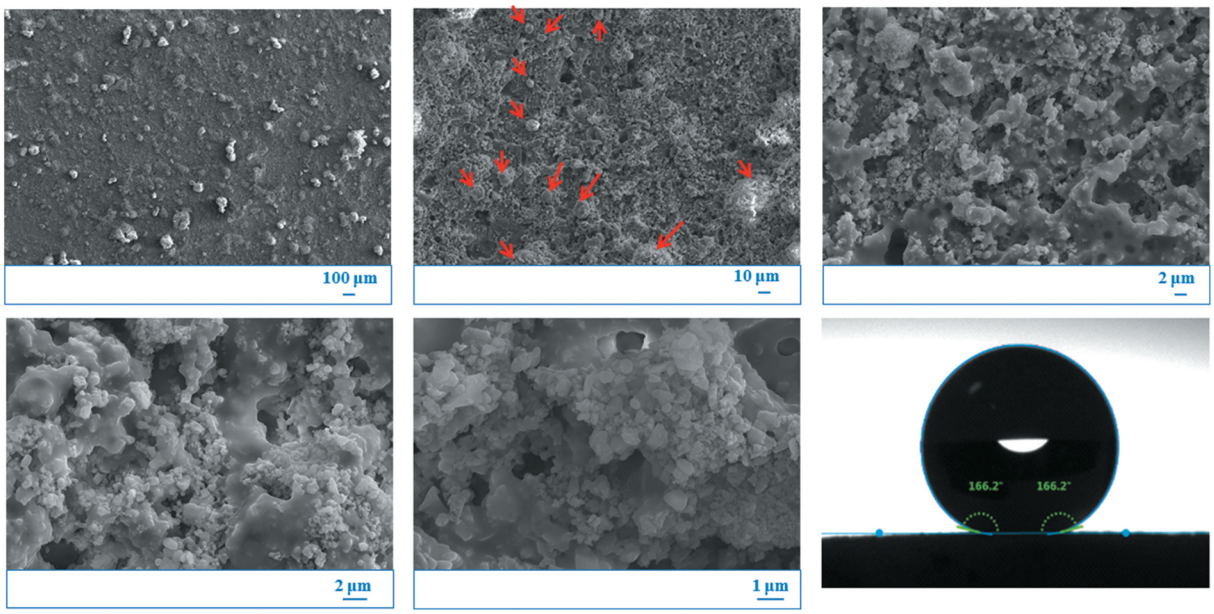

Figure 5. SEM-SE images of the tile surface with the SN-modified glaze and sintered at 980◦C for 5 min at various magnifications (red arrows indicates ball-like spherical granular structures).

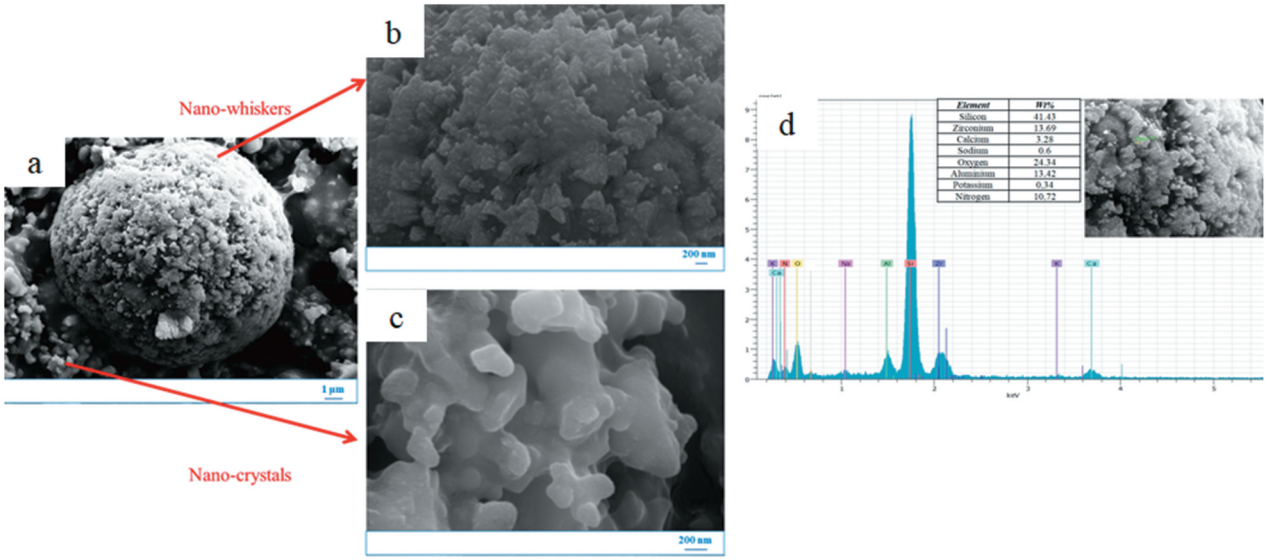

Figure 6. SEM-SE images show ball-like spherical granular structure and nano-scale crystals on the other regions (a-c), EDX spectra is taken from spherical balls (d).

For the samples sintered at 1050°C for 60 min, the surface has a high porosity content and pore sizes increased to 5–20 µm (Figure 7). Spherical granular structures have bigger sizes (20-50 µm). On the other hand, nano-sized rods which have a white color are available on the granular structures (yellow arrows indicate these structures). For this reason, the surface has a 154° high water contact angle, low surface energy of 1.58 mj/m^2 and a high roughness (Ra: 487 µm), with an ultra-water repellent feature.

The sample surface has a very porous structure with a wide range of pore size of 1–20 µm and 1-2 µm in granular structure if the sample is sintered at 1100°C for 5 minutes (Figure 8). The increase in porosity content and pore size may result in a decreasing contact angle from 154° to 138°. The nano-size rods, which have a white color, are present in the granular structures (yellow arrows indicate these structures). This structure is also present for the samples sintered at 1050°C for 60 min. Nano–rods are well developed with the increase in sintering temperature from 1050°C to 1100°C (Figure 9). The micro granules are of 1-2 micron diameter and the nano rods are of 100 nm in diameter.

When the sintering time increased to 60 min., pore size increased to ~50 µm, granular structures and nano-rods collapsed (Figure 10), and the superhydrophobic effect disappeared (θ = 68°). On the other hand, high-intensity C peaks can result from oxidation of silicon nitride in air at 1100°C for 60 min [31]. Silicon

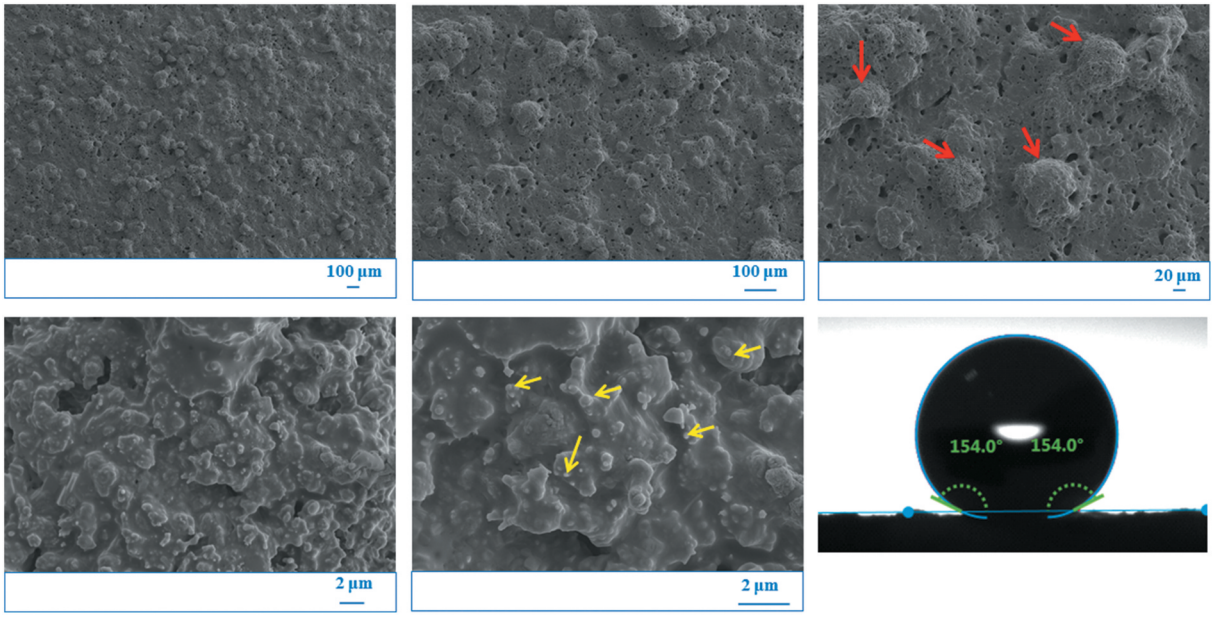

Figure 7. SEM-SE images of SN-modified glaze surfaces sintered at 1050◦C for 60 min at various magnifications (red arrows indicates ball-like spherical granular structures, yellow arrows indicate nano-rods).

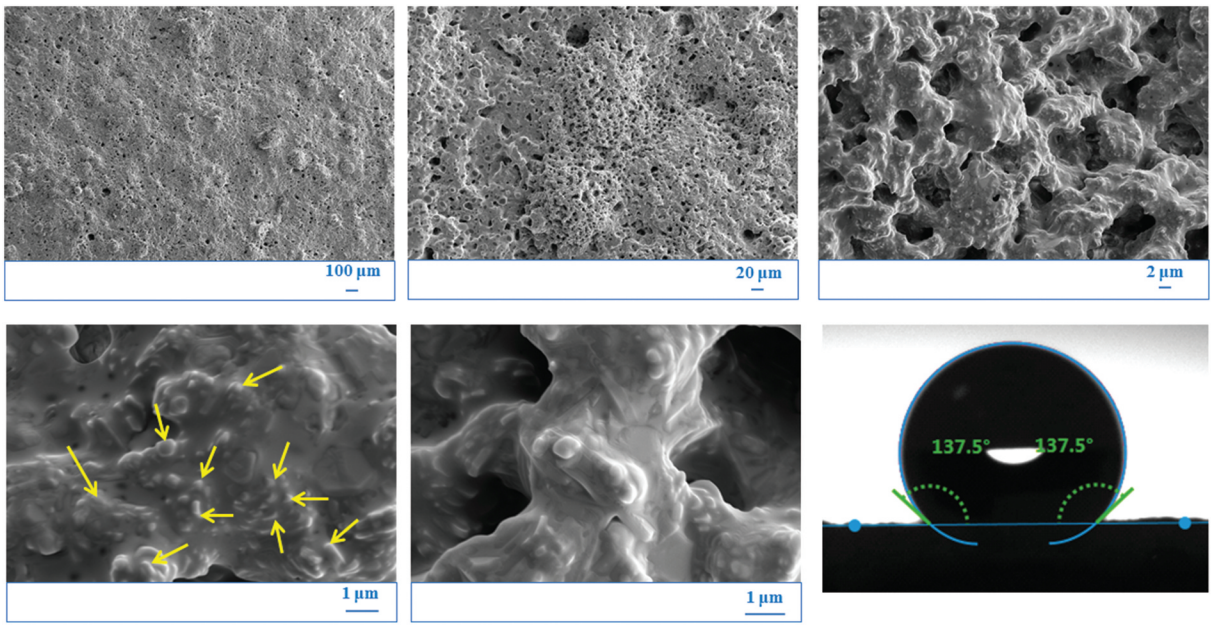

Figure 8. SEM-SE images of SN-modified glaze surfaces sintered at 1100◦C for 5 min at various magnifications (yellow arrows indicate nano-rods).

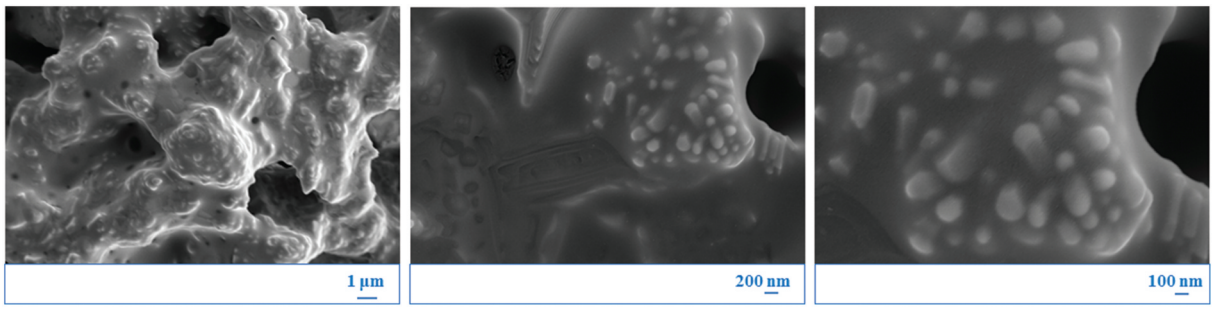

Figure 9. SEM image of micro-nano hybrid structures of surface which was sintered at 1100◦C for 5 min at various magnifications (15.000, 50.000, 100.000x).

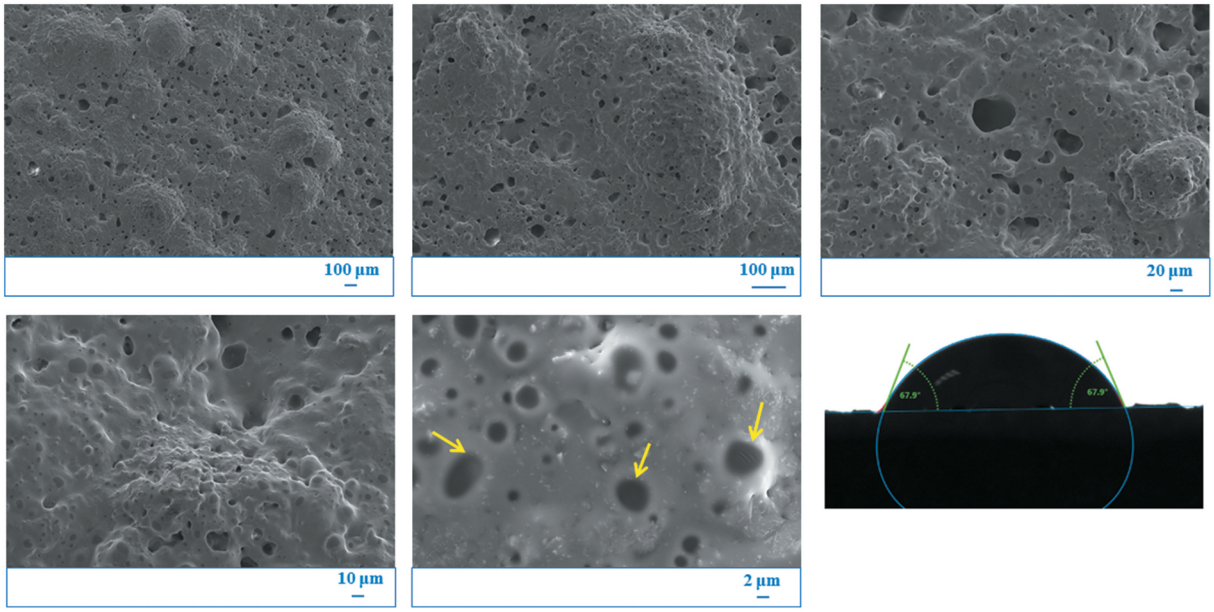

Figure 10. SEM-SE images of SN-modified glaze surfaces sintered at 1100◦C for 60 min. at various magnifications (arrows indicate pores resulted from bloating).

nitride is oxidized by oxygen to form C according to following equation:

$Si_3N_4 + 3\ O_2 \rightarrow 3\ SiO_2 + 2\ N_2$

Besides, bloating was observed when the sintering time increased to 60 min. (Figure 10d). Over firing is the main reason for the bloating problem.

The water contact angle of the Si_3N_4 modified glaze versus surface roughness Ra is given in Figure 11a. As can be seen from the graph, specific surface topography is effective in achieving high contact angles. For a Ra value between the 244 and 487 µm, the contact angle is changing between 138° to 166°. As can be seen from the SEM images, when the samples are sintered at 980°C and 1050°C, spherical ball-like granules are present but with different sizes (0.5–10 and 5-20 µm, respectively). Increase in granule size results in higher surface roughness. With further increase in sintering temperature, these spherical ball-like granules disappeared and very fine micron-sized mounds grow with nanoscale rods in these structures. The surface roughness values are very close when the samples are sintered at 1100°C for 5 (Ra: 352 µm). With further increase in sintering time to 60 min., micro-nano hybrid structures disappeared, pore sizes enlarged, the bloating problem is observed and roughness is decreased to 140 µm. This type of surface has a 68° water contact angle. The reduction in contact angle is related to surface roughness and surface topography which induced by Si_3N_4. The surface energies of the polymer coated Si_3N_4 modified ceramic surfaces obtained by sintering at different sintering regimes are correlated with the contact angles (Figure 11b). The lower surface energies (1.3– 1.58 mJ/m^2) caused higher contact angles (154-166°). When the surface energy is 14.35 mJ/m^2, the surface shows a hydrophobic character (CA: 138°). If the surface energy is 61.24 mJ/m^2, the water contact angle was further decreased and was down to 68° with a hydrophilic nature. Thus,

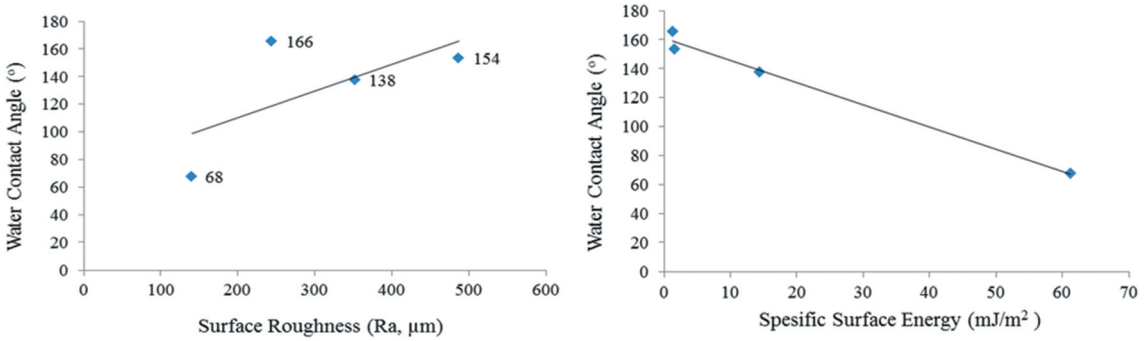

Figure 11. The contact angles of the polymer coated SN modified glazed surfaces versus (a) surface roughness parameter, (b) specific surface energy.

as empirically shown, reduction of surface free energy was necessary to obtain a superhydrophobic surface in accordance with theoretical considerations.

In this study, the contact angle exceeds 160° and the hysteria ($\Delta\Theta$) gets close to zero thanks to the synergistic effect resulting from the use of the glaze mixture containing β-Si_3N_4 powder with the coating solution. After the water drop touches the surface, it does not bounce on the surface. Therefore, hysteria is very low (~0-3°) and has a self-cleaning feature. Furthermore, the resistant surfaces having high wearing resistance can be achieved by means of inorganic surface modification, which is provided by adding β-Si_3N_4 powder into the glaze mixture thanks to the high covalent bonds between the Si and N atoms, and as well it maintains features longer than the equivalents thereof.

4. Conclusions

Superhydrophobic ceramic surfaces are developed by adding β-Si_3N_4 powder in wall tile glaze slurry. The glazed surfaces rich in β-Si_3N_4 phase present a micro-nano hybrid structure due to the whisker/rod-like nano β-Si_3N_4 crystals on the micron–sized granules. It was observed that sintering regime has influence on the formation of such a specific surface morphology. The highest contact angle achieved was 166° for the tiles fired at 980°C for 5 min. For a sintering temperature between 980°C and 1050°C and a dwell time between 5 and 60 minutes, the contact angles of formed surface are superhydrophobic (154-166°). When the dwell time was 60 minutes and the sintering temperature was 1100°C, the contact angle dropped abruptly to 68° and showed a hydrophilic character. This phenomenon can be related mainly due to surface morphology and was confirmed by SEM images. The surface morphology affects the surface energy rather than polymer coating.

Acknowledgments

The corresponding author (N. Calis Acikbas) would like to thank UNESCO-Loreal funding Support Scholarships for Young Woman Scientists Award. The authors of this study would like to thank BİEN Ceramic company for their cooperation and supply of the necessary raw materials.

The Authors' Biography

Nurcan Calis Acikbas born in 1980, received BSc, MSc and PhD Degrees in Ceramic Engineering from Anadolu University, Turkey in 2002, 2004 and 2009, respectively. During her graduate study, as a visiting scholar, she had been to many prestigious institutions including Jožef Stefan Institute, Institute of Inorganic Chemistry Slovak Academy of Sciences, Kanpur-Indian Technology Institute and Indian Glass and Ceramic Research Center. She was Manager at MDA Advanced Ceramics Ltd. from 2004 to 2010. In 2010, she joined the Bilecik University. She became the Head of Mechanical and Manufacturing Engineering Department in 2014 and 2015, Founding Head of Metallurgical and Materials Engineering Department between 2015 and 2018, Deputy Director of Bilecik University Central Research Laboratory between 2011 and 2014. Her PhD thesis was awarded as the most successful University-Industry Collaboration Thesis of Technology Development Foundation of Turkey in 2012. As an active researcher, she has been coordinator and/or researcher of many scientific projects including UNESCO, San-Tez, TUBITAK-ARDEB, TUBITAK-TEYDEB, TUBITAK-International Joint Projects. Dr. Açıkbaş also received UNESCO-Loreal Young Woman Scientist Award of 2014 for her prestigious research project. She has been an active member of Turkish Ceramic Society, European Ceramic Society and the founding member of Bilecik University-Industry Collaboration Society. She has been a member of TUBITAK Advisory Board since February 2019. Her current research interest is structure-property relationships, tribology, silicon nitride-based ceramics and its applications. She is currently working at Mersin University, Engineering Faculty, Department of Metallurgical and Material Engineering Department.

Assoc. Prof. Dr. Gokhan Acikbas, born in 1979, studied Materials Science and Engineering with specialization in characterization of ceramics and polymer matrix composites. He received B.S., M.S. degrees in Ceramic Engineering from Anadolu University and Ph.D. degrees in Materials Science and Engineering in Turkey in 2002, 2007 and 2016, respectively. He was with TÜBİTAK Ceramic Research Center from 2003 to 2008 and Eczacıbaşı Vitra Company from 2008 to 2011. Since 2011, he has been working at Bilecik Seyh Edebali University.

Author contributions

Nurcan Calis Acikbas: Conceptualization, Methodology, Investigation, Writing, Visualization, Supervision, **Gokhan Acikbas**: Conceptualization, Methodology, Validation, Investigation, Visualization, Resources.

Disclosure statement

No potential conflict of interest was reported by the author(s).

Funding

This work was supported by the UNESCO-TURKEY [2014].

ORCID

Nurcan Calis Acikbas http://orcid.org/0000-0001-6193-8252

References

[1] Johnson ER, Dettre HR, Contact angle hysteresis I. Study of and idealized rough surface, Advances in Chemistry Series, 43 (1964) 112–135.

[2] Neinhuis C, Barthlott W. Characterization and distribution of water-repellent, self-cleaning plant surfaces, Ann. Botany. 1997;79:667–677.
[3] Atsushi H, Osamu T. Preparation of ultra water-repellent films by microwave plasma-enhanced CVD. Thin Solid Films. 1997;303(1–2):222–225.
[4] Nakajima A, Abe K, Hashimoto K, et al. Preparation of hard super-hydrophobic films with visible light transmission. Thin Solid Films. 2000;376(1–2):140–143. https://doi.org/10.1016/S0040-6090(00)01417-6
[5] Wang X, Chen L, Wang L, et al. Synthesis of novel nanomaterials and their application in efficient removal of radionuclides. Sci China Chem. 2019;62 (8):933–967.
[6] Zhang X, Shi F, Yu X, et al. Polyelectrolyte multilayer as matrix for electrochemical deposition of gold clusters: toward super-hydrophobic surface. J Am Chem Soc. 2004;126(10):3064–3065.
[7] Han J, Jang Y, Lee D, et al. Fabrication of a bionic superhydrophobic metal surface by sulfur-induced morphological development. J Mater Chem. 2005;15 (30):3089–3092.
[8] Woodward I, Schofield WCE, Roucoules V, et al. Superhydrophobic surfaces produced by plasma fluorination of polybutadiene films. Langmuir. 2003;19 (8):3432–3438. https://doi.org/10.1021/la020427e
[9] Erbil HY. Transformation of a simple plastic into a superhydrophobic surface. Science. 2003;299 (5611):1377–1380.
[10] Han J, Lee D, Ryu C, et al. Fabrication of superhydrophobic surface from a supramolecular organosilane with quadruple hydrogen bonding. J Am Chem Soc. 2004;126(15):4796–4797. https://doi.org/10.1021/ja0499400
[11] Latthe SS, Terashima C, Nakata K, et al. Superhydrophobic surfaces developed by mimicking hierarchical surface morphology of lotus leaf. Molecules. 2014;19(4):4256–4283.
[12] Zhai L, Cebeci FC, Cohen RE, et al. Stable superhydrophobic coatings from polyelectrolyte multilayers. Nano Lett. 2004;4(7):1349–1353.
[13] Wu X, Zheng L, Wu D. Fabrication of superhydrophobic surfaces from microstructured ZnO-based surfaces via a wet-chemical route. Langmuir. 2005;21 (7):2665–2667. https://doi.org/10.1021/la050275y
[14] Cacciotti I, Nanni F, Campaniello V, et al. Development of a transparent hydrorepellent modified SiO_2 coatings for glazed sanitarywares. Mater Chem Phys. 2014;146(3):240–252.
[15] Reinosa JJ, Romero JJ, Miguel A, et al. Inorganic hydrophobic coatings: surfaces mimicking the nature. Ceram Int. 2013;39(3):2489–2495.
[16] Määttä J, Piispanen M, Kuisma R, et al. Effect of coating on cleanability of glazed surfaces. J Eur Ceram Soc. 2007;27(16):4555–4560.
[17] Kuisma R, Fröberg L, Kymäläinen HR, et al. Microstructure and cleanability of uncoated and fluoropolymer, Zia and titania coated ceramic glazed surfaces. J Eur Ceram Soc. 2007;27(1):101–108.
[18] Özcan S, Açıkbaş G, Çalış Açıkbaş N. Induced superhydrophobic and antimicrobial character of zinc metal modified ceramic wall tile surfaces. Appl Surf Sci. 2018;438:136–146.
[19] Huang J, Huang Z, Liu Y, et al. β-Sialon nanowires, nanobelts and hierarchical nanostructures: morphology control, growth mechanism and cathodoluminescence properties. Nanoscale. 2013;6 (1):424–432.
[20] Rosso M, (2009). Modification of silicon nitride and silicon carbide surfaces for food and biosensor applications. PhD thesis submitted to Wageningen University.
[21] Batha HD, Whitney ED. Kinetics and mechanism of the thermal decomposition of Si3N4. J Am Ceram Soc. 1973;56(7):365–369. https://doi.org/10.1111/j.1151-2916.1973.tb12687.x
[22] Açıkbaş G Thesis, Developments of micromorphology on ceramic surfaces, Anadolu University, (2007)
[23] Açıkbaş G, Özcan S, Çalış Açıkbaş N, Formation of Superhydrophobic Character on Ceramic Surfaces, 2nd International Symposium on Innovative Technologies in Engineering and Science (2014) 606–613, https://www.isites.info/pastconferences/isites2014/isites2014/papers/A16ISITES2014ID98.pdf
[24] Fowkes FM. Attractive forces at interfaces. Ind Eng Chem. 1964;56(12):40–52.
[25] Owens D, Wendt R. Estimation of the surface free energy of polymers. J Appl Polym Sci. 1969;13 (8):1741–1747.
[26] Kaelble DH. Dispersion-polar surface tension properties of organic solids. J.Adhes 1970;2(2):66–81.
[27] Herring C. Effect of change of scale on sintering phenomena. J Appl Phys. 1950;21(4):301–303. https://doi.org/10.1063/1.1699658
[28] Hunger A, Carl G, Gebhardt A, et al. Ultra-high thermal expansion glass–ceramics in the system MgO/Al2O3/TiO2/ZrO2/SiO2 by volume crystallization of C. J Non-Crystalline Solids. 2008;354 (52–54):5402–5407.
[29] Deng Y, Xu L, Lu H, et al. Direct measurement of the contact angle of water droplet on Q in a reservoir rock with atomic force microscopy. Chem Eng Sci. 2018;177:445–454.
[30] Raider SI, Flitsch R, Aboaf JA, et al. Surface oxidation of silicon nitride films. J Electrochem Soc. 1976;123 (4):560. https://doi.org/10.1149/1.2132877
[31] Mieskowski DM, Sanders WA. Oxidation of Silicon Nitride Sintered with Rare-Earth Oxide Additions. J Am Ceram Soc. 1985;68(7):C–160.